Hydraulic Control of a Highly Stratified Estuarine Front*

DANIEL G. MACDONALD+

Massachusetts Institute of Technology/Woods Hole Oceanographic Institution Joint Program in Oceanography/Applied Ocean Science and Engineering, Cambridge, Massachusetts

W. ROCKWELL GEYER

Woods Hole Oceanographic Institution, Woods Hole, Massachusetts

(Manuscript received 23 June 2003, in final form 23 June 2004)

ABSTRACT

Observations at the mouth of the Fraser River (British Columbia, Canada) indicate an abrupt frontal transition between unstratified river outflow and a highly stratified river plume with differences in salinity greater than 25 psu across a few meters in the vertical direction and several hundred meters in the horizontal direction. The front roughly follows a natural break in the bathymetry, crossing the channel at an angle of approximately 45°, and is essentially stationary for a period of approximately 3.5 h centered on the low tide following the larger of two daily ebbs. The location of the front is coincident with observations of significantly supercritical internal Froude numbers at the front, based on velocities in the along-flow direction. This observation contradicts the one-dimensional theory, which indicates that the Froude number should be 1. However, because the front is oriented obliquely to the outflow, a coordinate system can be selected that is normal to the front and for which a critical Froude number of 1 is obtained. This indicates that a Froude angle, similar in application to a Mach angle for transonic flows, can be used to determine critical conditions when the front is oblique to the principal flow direction.

1. Introduction

In uniform-density flows, the concept of hydraulic control provides a means of relating discharge to flow depth (e.g., Henderson 1966, p. 41). This concept has been extended to two-layer flows (Armi 1986; Dalziel 1991), and the hydraulic control of one-dimensional arrested fronts and exchange flows has been well described analytically by Armi and Farmer (1986) and Farmer and Armi (1986) for contractions and sills, respectively. The concept of hydraulic control can be useful in oceanographic applications for evaluating natural exchange flows (e.g., Farmer and Armi 1988; Armi and Farmer 1988) and for predicting the location of density fronts (e.g., Benjamin 1968). However, environmental flows are rarely one-dimensional, and the direct application of one-dimensional theories to these flows may leave out important aspects of the dynamics.

The condition of an arrested front can be considered the limiting case of a two-layer exchange flow in which flow in one of the layers has been reduced to zero. Benjamin (1968) obtained a solution for an arrested front in a uniform channel with the frontal condition

$$\frac{U_o^2}{g'h_o} = \frac{1}{4}, \tag{1}$$

where U_o represents the mean velocity in the channel immediately upstream of the front, h_o is the channel depth, and $g' = g(\rho_1 - \rho_2)\rho_o^{-1}$ is a reduced gravity, with the subscripts 1 and 2 referring to the upper and lower layers, respectively. Armi and Farmer (1986) and Farmer and Armi (1986) considered a similar problem, but in which there was a variation in width or depth of the channel. The arrested-front condition for their formulation is

$$\frac{U_o^2}{g'h_o} = 1. \tag{2}$$

The difference between this relation and the Benjamin solution is due in part to the use of the hydro-

* Woods Hole Oceanographic Institution Contribution Number 11217.

+ Current affiliation: School for Marine Science and Technology, University of Massachusetts, Dartmouth, New Bedford, Massachusetts.

Corresponding author address: Daniel MacDonald, School for Marine Science and Technology, University of Massachusetts, Dartmouth, 706 South Rodney French Boulevard, New Bedford, MA 02744-1221.
E-mail: dmacdonald@umassd.edu

static approximation (i.e., the neglect of vertical accelerations at the front) in Armi and Farmer's analysis. This approximation is valid at scales of flows in the ocean and estuaries in which changes in cross-sectional area occur over horizontal scales significantly greater than the vertical scale of the flow.

A typical one-dimensional frontal region, resembling the idealization of Farmer and Armi (1986), is portrayed in Fig. 1. Here, near-field and far-field regions are delineated, based on the shape of the interface, and the frontal zone is identified. In Fig. 1, a sharp interface between the two layers is shown, although field observations typically identify an interface of some finite width across which the transition between water masses occurs. The front and near field of the plume compose a region that will be further referred to as the "lift-off" zone because across this zone the river discharge loses contact with the bottom and the interface rises rapidly in the seaward direction.

Seaward of the front, the flow is supercritical, and the composite Froude number, which can be defined as

$$G^2 = F_1^2 + F_2^2, F_i^2 = \frac{U_i^2}{g' H_i}, \tag{3}$$

is greater than 1. Here F represents the individual layer Froude numbers, and the subscript i is used to identify the layers. In the inviscid theory of Armi and Farmer there is no flow in the lower layer, and so the only contribution to the composite Froude number is the upper-layer Froude number, which approaches 1 at the toe of the front. Hence, the Armi and Farmer frontal condition can also be considered a critical Froude number condition, although the density contrast and thus g' are defined by the conditions in the two-layer flow seaward of the front.

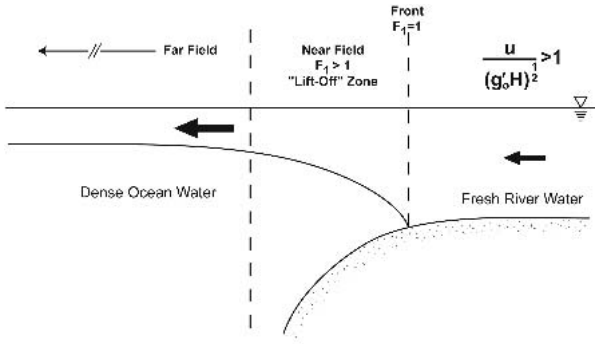

FIG. 1. Definition sketch for front and near-field regions. Fresh river water is discharging to the ocean, establishing a front at the point where the upper-layer Froude number, F_1, is equal to 1. The region immediately seaward of the front where the depth of the interface is adjusting rapidly and Froude numbers are supercritical is considered to be the near-field region and is sometimes referred to as the "lift off" zone. The far field lies seaward of this adjustment region and extends far downgradient. The near-field physics are dominated by inertial influences. Buoyancy differences and external forcing (e.g., wind stress) dominate in the far field. In the region landward of the front, the ratio of velocity to a wave speed representative of the density difference at the front is greater than 1. This illustrates that the location of the front is pushed sufficiently downslope to satisfy the critical condition.

The Armi and Farmer frontal condition is consistent with observations of estuarine fronts in several previous studies of highly stratified estuaries, including the Mississippi River estuary (Wright and Coleman 1971) and the Ishikari River estuary (Kashiwamura and Yoshida 1978). However, observations and numerical model results from the Hudson Estuary (Geyer et al. 1998) suggest that fronts may occur at significantly supercritical conditions (i.e., $U_o^2 > g' h_o$). The front observed in the Hudson Estuary was found to be oriented obliquely to the flow direction, and the deviation from the Armi and Farmer theory suggests that a two-dimensional approach to frontal dynamics may be required.

A two-dimensional approach has been undertaken for the description of hydraulic control in unstratified open channel flows (Ippen 1936) and with respect to the surface frontal structure of estuarine plumes (Garvine 1982). However, multidimensionality has not been considered in application to the hydraulics of salt wedge fronts. This study provides observational evidence that two-dimensional effects need to be considered to properly define the frontal conditions in an estuarine front, based on observations from a highly stratified front at the mouth of the Fraser River, British Columbia, Canada, during the summer freshet.

2. The Fraser Estuary and the 2000 field effort

The Fraser River Estuary is located at the mouth of the Fraser River, which flows into the Strait of Georgia in the southwestern corner of British Columbia, approximately 20 km south of the City of Vancouver (Fig. 2). With a mountainous watershed that encompasses 234 000 km^2, the Fraser River is the dominant source of freshwater to the inland sea created by the Strait of Georgia, the Strait of Juan de Fuca, and Puget Sound. The freshet in the Fraser typically occurs in late May or June as snowpack at the higher elevations of the inland mountains begins to melt. Peak freshwater discharge during the freshet is on the order of 10^4 m^3 s^{-1}.

The mouth of the Fraser River consists of a channel confined by a jetty along its northern boundary, with shallow tidal flats to the south, and an average channel depth on the order of 10–15 m, as shown in Fig. 2. The jetty along the northern portion of the channel ends at Sand Heads, allowing lateral expansion of outflow to the north. On the south side, tidal flats continue 1.5 km seaward beyond Sand Heads. Approximately 0.5–1 km beyond Sand Heads the bathymetry breaks sharply, reaching depths greater than 50 m in less than 500 m in the along-channel direction. This bathymetric break is situated at an angle of roughly 45° to the channel, and the foreslope is characterized by an irregular pattern of gullies with scales on the order of hundreds of meters.

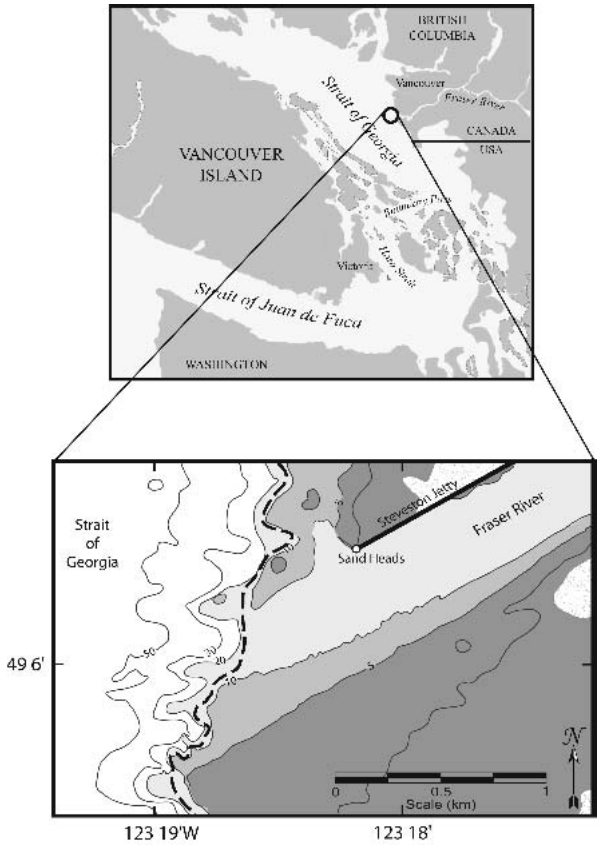

FIG. 2. Locus and mouth of the Fraser River estuary. In the bottom panel, the thick dashed line represents the location of the 12-m bathymetric contour, which serves as a marker for the bathymetric break. Contours are shown in meters and are based on a compilation of bathymetric data from the Canadian Hydrographic Service (Chart 3490, 1997) and shipboard measurements (Jul 2002).

Energetic tides in the Strait of Georgia, characterized by amplitudes typically ranging from 2.5 to 4.0 m with a pronounced diurnal component, combine with the influx of buoyancy and inertia from the river discharge to create a highly energetic estuarine environment and intense stratification. The resulting salt wedge is characterized by salinity differences of greater than 20 psu across only a few meters in the vertical direction and less than 500 m horizontally at the head. This salt wedge advances landward some 15–20 km into the channel on each tidal cycle, only to be flushed back to the mouth daily during the strong ebb (Geyer and Farmer 1989). At this point in the cycle, after the salt wedge has retreated to the mouth, there is a period of quasi steady-state dynamics as the front location remains stable for several hours prior to beginning its next advance into the channel on the flooding tide. This paper focuses on the structure of the lift-off zone during this stationary period.

The 2000 study was timed to coincide both with the freshet and spring tides and was conducted between 30 June and 4 July 2000. Data were collected from shipboard instrumentation, including two hull-mounted ADCPs, operating at 1200 and 300 kHz, and a towed Ocean Sensors 200 Series CTD unit. Three to five parallel passes, oriented in the along-channel direction and spaced evenly across the channel, were used to identify the three-dimensional structure of the lift-off zone. Strong velocities in the along-channel direction precluded the towing of instruments on cross-channel transects. The seaward extent of the data transects rarely exceeded 2 km beyond Sand Heads, as the focus of the study was confined to the front and the near field of the plume.

3. Structure of the lift-off zone

Data from five passes during the late ebb on 30 June were used to construct upper-layer streamlines for the lift-off region, as shown in Fig. 3. Velocity data from the five passes were interpolated laterally by using an elliptical interpolation scheme with a major axis at the angle of the bathymetry break (see the appendix). Following horizontal interpolations, streamlines were generated from velocities averaged vertically across all fluid with salinity less than 20 psu. The direction of the streamline was defined parallel to the mean velocity at each point such that the mean cross-streamline velocity was equal to zero. A new coordinate system was generated from the established streamlines by defining normal grid lines, as shown on Fig. 3, and measuring distances along the deformed streamline-normal grid mesh.

The three-dimensional structure of the lift-off zone is illustrated with a series of cross sections. Eight sections through the lift-off zone are indicated on Fig. 3, four of them in the along-channel direction (shown in Fig. 4) and four in the cross-channel direction (shown in Fig. 5). The series of along-channel sections shown in Fig. 4 indicate that stratification is high and relatively uniform across the channel. This is evidenced by the similarly close spacing of the isohalines in each panel. The frontal zone itself is defined by the bottom intersection of the isohalines and is well constrained across most of the channel (sections 1–3), but somewhat broader toward the north. Note that in all cases, the seaward edge of the frontal zone is anchored very near the bathymetric break and that it is the landward edge of the frontal zone that varies.

The cross-channel sections of Fig. 5 demonstrate the inclination of the isohalines, which slope upward to the north across most of the width of the frontal zone. The velocity also shows significant lateral structure with a high velocity region in the center of the plume that widens and shoals in the seaward direction. The cross-channel velocity structure is strongly sheared with surface flows directed northward and deeper flows moving toward the south. The southward flow beneath the

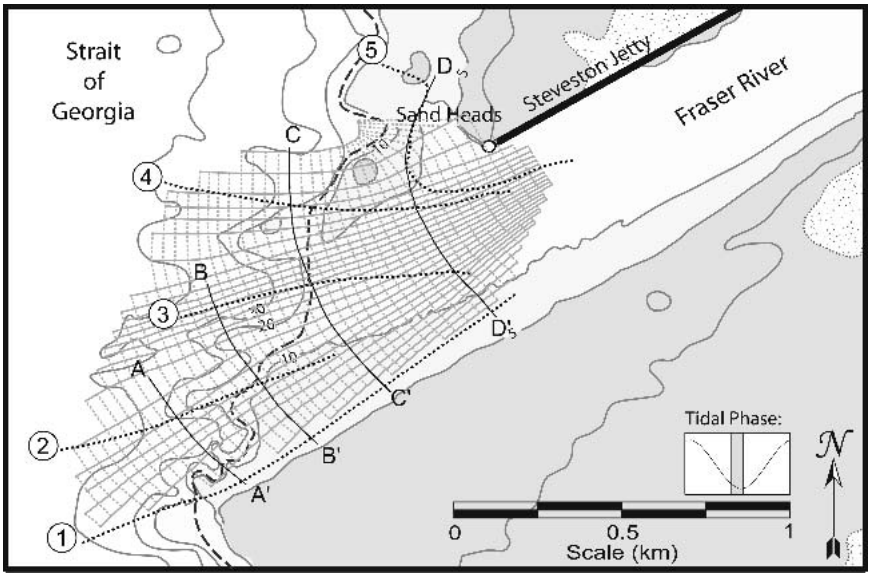

FIG. 3. Mouth of the Fraser, showing upper-layer streamlines and the location of cross sections shown in Figs. 4 and 5. Streamlines are shown as the solid gray lines, and cruise tracks are identified as the heavier dotted lines. The heavy dashed line delineates the location of the 12-m isobath and the approximate location of the bathymetric break. Cruise tracks numbered 1–4 are shown in cross section in Fig. 4. Transverse cross sections A–A′ through D–D′ are shown in Fig. 5. Streamlines are generated from ADCP velocity data collected along the identified cruise tracks. Data were collected during the late ebb, as shown in the inset frame. Streamline normals are shown behind the streamlines and, together with the streamlines, create a natural curvilinear coordinate system.

plume is associated with the ebbing tide in the Strait of Georgia, coincident with the ebb in the Fraser Estuary.

As indicated in Fig. 4, the bottom front is relatively compact in the along-channel direction. This is illustrated again on Fig. 6, where the frontal zone for the lift-off period is delineated by the width of the region where water with salinities of 5–20 psu intersects the bottom. The shaded region in Fig. 6 is based on observations from several different days, and the width may be overestimated because of the horizontal resolution of the CTD tow-yo passes, as indicated by the dotted lines in Fig. 4.

One of the striking characteristics of the frontal zone is its oblique orientation with respect to the channel and the alongstream direction. The front is approximately parallel with the bathymetry across the southern portion of the channel but diverges from the isobaths to the north where it curves eastward toward Sand Heads and attaches to the Steveston Jetty.

The accumulated data used to generate Fig. 6 span across several hours of the tidal cycle and are compiled from observations on several different days. To evaluate temporal variations in the frontal location within this dataset, all front locations observed during the 5-day field study, within the 3-h period each day centered on the low tide following the largest daily ebb, were compared with respect to lateral position within the channel. Changes in frontal position during the lift-off period correspond with a mean velocity on the order of 50 m h^{-1} (0.014 m s^{-1}) but with large fluctuations between individual ship tracks; these variations are more likely due to lateral variability in the front position rather than fluctuating frontal velocities. In any case, the net frontal velocity is negligible relative to the velocity of the freshwater outflow during the lift-off period, which is on the order of 2 m s^{-1}.

The momentum equations for the upper and lower layer can be combined to form a single equation for the two-layer system (e.g., Geyer and Farmer 1989). An analysis of terms in this combined momentum equation indicates that, during the lift-off period, the momentum balance is quasi steady. The temporal acceleration terms can be estimated by comparing the data shown on Fig. 4 with similar data from collocated passes repeated approximately 2–3 h later. The net acceleration of the upper layer during this period was on the order of 10^{-4} m s^{-2}, with similar values seen in the lower layer. These accelerations are more than an order of magnitude smaller than the convective acceleration term associated with the upper layer, which is on the order of 3×10^{-3} m s^{-2}, suggesting that the system can safely be considered quasi steady.

4. Control of the front

Composite Froude numbers were calculated for the lift-off region using a depth-averaged, upper-layer ve-

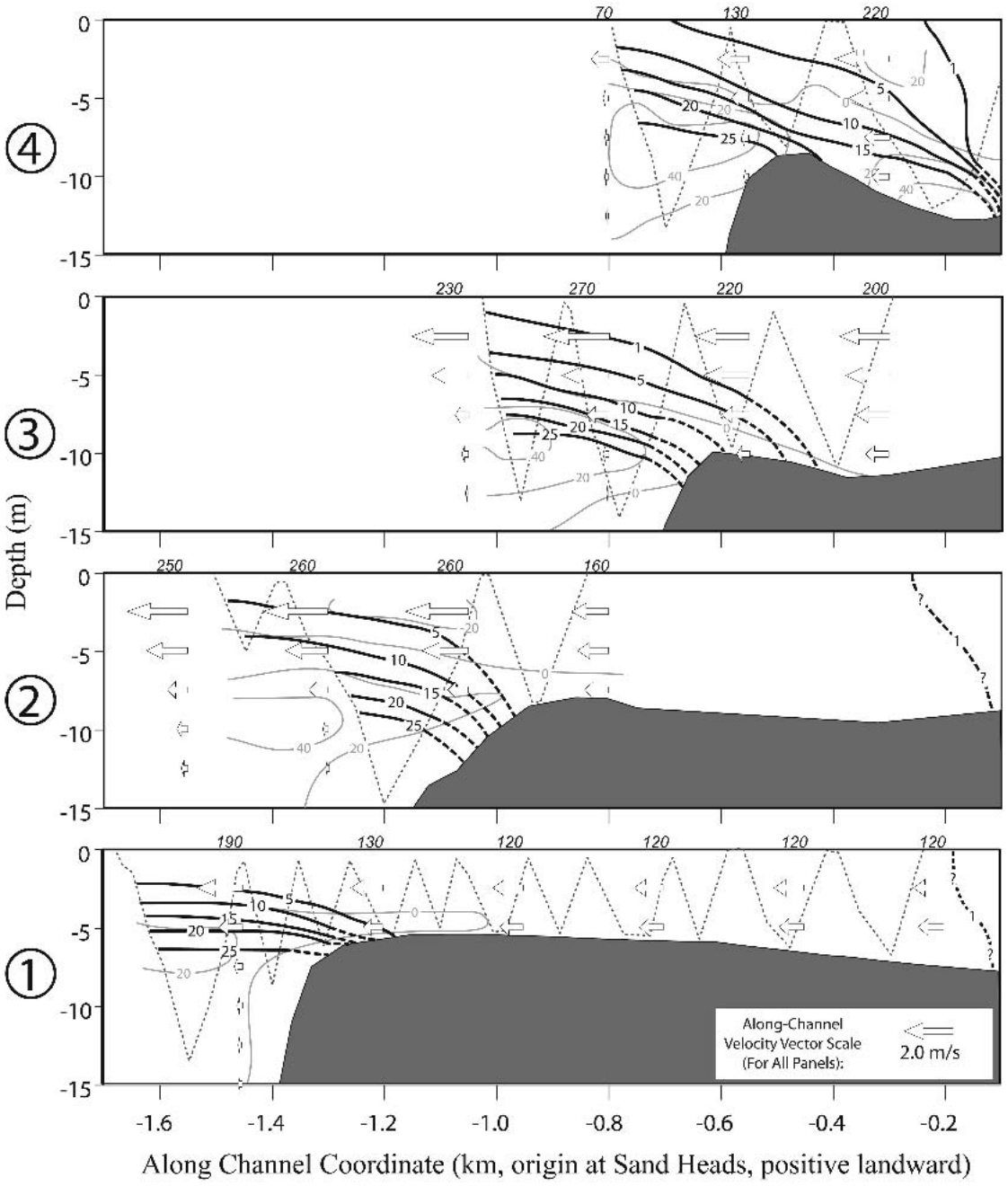

FIG. 4. Along-channel cross sections through the lift-off zone along cruise tracks as shown in Fig. 3. Salinity contours (1, 5, 10, 15, 20, and 25 psu) are shown in black, with arrows representing the magnitude and direction of the streamwise velocity component. The numbers above each panel represent the magnitude of the uppermost velocity vectors shown (cm s^{-1}). Cross-channel velocity (i.e., along the streamline normals shown dotted in Fig. 3) is represented by the gray contours (cm s^{-1}), with positive values representing southward-directed flows. The dotted line represents the approximate path of the towed CTD unit.

locity. Values for the upper 2 m of the water column, where measurements from the hull-mounted ADCPs were unavailable were extrapolated based on a parabolic fit, satisfying the observed shear below two meters and an assumed shear of zero at the surface. The Froude numbers were based on velocities aligned in the direction of the upper-layer streamlines, as they were calculated using the total magnitude of the depth-averaged velocity vector. The calculations assumed a layer interface coincident with the 14-psu isohaline surface, which represents the midpoint of the salinity range (0–28 psu). Lower-layer streamwise velocities are

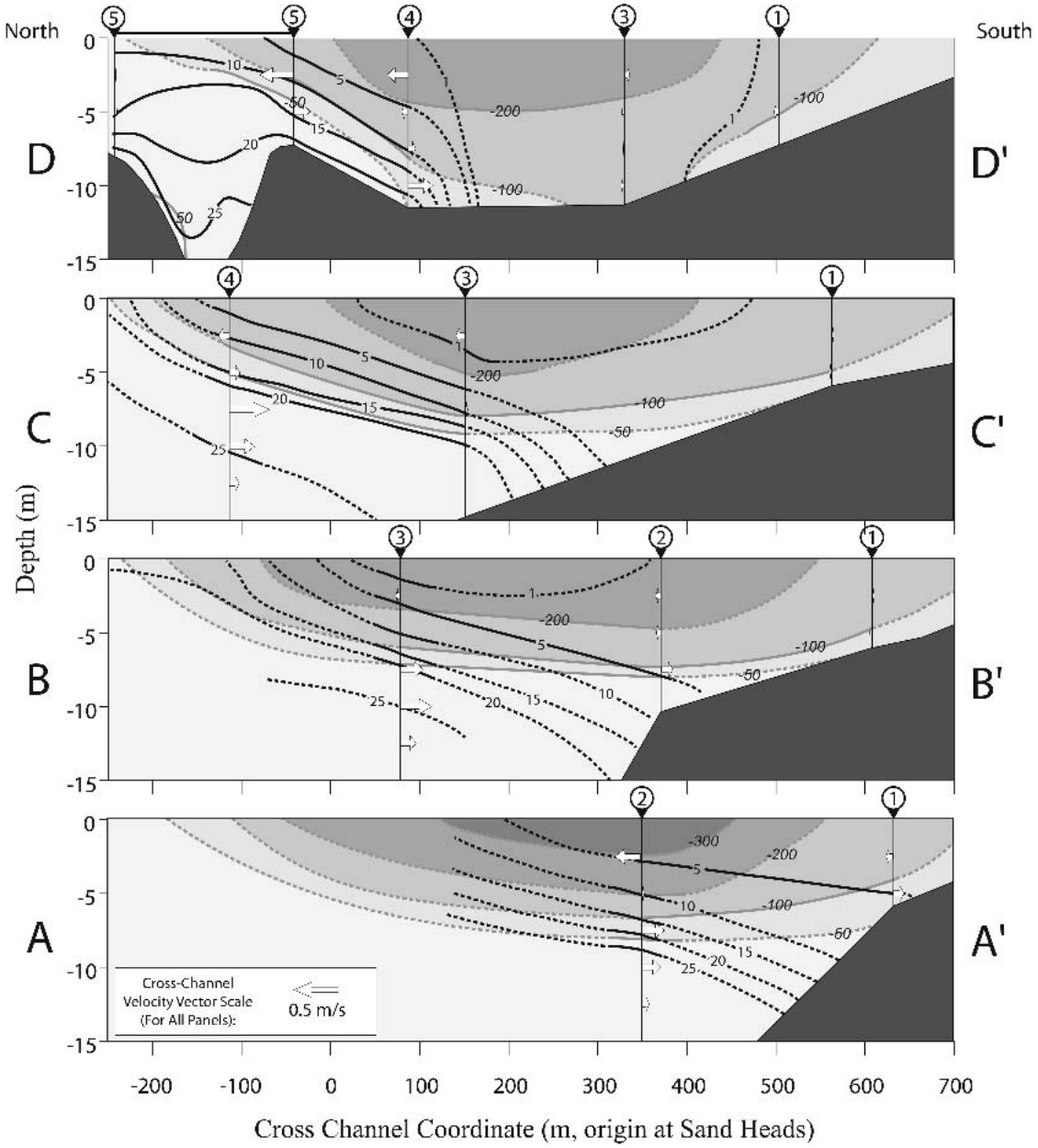

FIG. 5. Transverse channel cross sections through the lift-off zone at progressively seaward positions as identified by the cross-section locations in Fig. 3. The ordinate axis represents cross-channel distance, in meters, from an origin aligned with Sand Heads. Positive values are directed in a generally southward direction (normal to the Steveston Jetty). Salinity contours (1, 5, 10, 15, 20, and 25 psu) are shown in black, with arrows representing the magnitude and direction of the cross-channel velocity component (i.e., along the streamline normals shown dotted in Fig. 3). Streamwise velocity is represented by shading and contours (cm s^{-1}). The black triangles and numbers at the top of each cross section indicate the location and number of the cruise tracks from which data for these cross sections are extracted. The region between the two connected triangles in cross section D–D′ lies along a cruise track, as shown in Fig. 3. Dashed lines represent visual extrapolations of the observed data.

small, generally at least an order of magnitude smaller than upper-layer velocities, yielding lower-layer Froude numbers much less than 1 and a composite Froude number essentially equal to the upper-layer Froude number. Thus, velocities in the lower layer play an insignificant role with respect to two-layer hydraulics.

Regardless of small differences between mean upper-layer and lower-layer densities throughout the region, Froude numbers were calculated using a constant value of g' equal to approximately 0.15 m s^{-2}, which corresponds to a salinity difference of 20 psu. Landward of the front, "virtual" upper-layer Froude numbers were

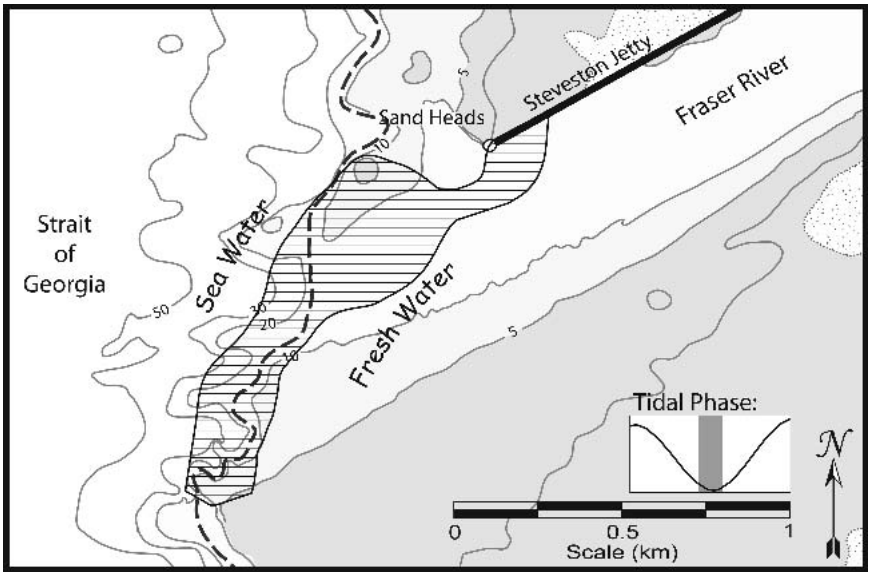

FIG. 6. Width of frontal zone as defined by presence of bottom water between 5 and 20 psu during the lift-off period as shown in the tidal curve inset. The hatched region is based on data observed during multiple passes through the lift-off zone between 30 Jun and 3 Jul 2000. For each pass, the landward edge of the region was represented by the most seaward bottom-water sample with salinities less than 5 psu. The seaward edge is defined by the most landward observation of water with a salinity greater than 20 psu at any point in the water column. The limits of the frontal zone are drawn liberally to encompass the observed front locations, and without regard to local bathymetry.

calculated using the same value of g' (0.15 m s^{-2}) and the total water depth, indicating what the Froude number would be if the front were located at that point. This approach provides a continuous representation of the Froude number across the front. The results of these calculations are shown in Fig. 7, where contours of the upper-layer Froude number are plotted across the lift-off zone using data from 30 June 2000.

The contours shown in Fig. 7 indicate that the flow is supercritical across the entire lift-off region, with a Froude number in the vicinity of 1.5 at the front across the majority of the channel. Supercritical velocities occur significantly landward of the front near the end of the confined channel at Sand Heads. These observations represent a significant departure from an expected Froude number equal to unity at the front. Prior to exploring the implications of these observations, a review of the calculations and alternative methods for interface determination, as well as the effects of bottom friction, velocity shear, and mixing on hydraulic theory, is warranted.

a. Interface height determination

It is possible that the 14-psu isopycnal does not adequately describe the dynamically important surface approximating the sharp distinction between two distinct layers and that a different isopycnal, or some other means of identifying the transition between water masses, should be used. As an alternative to selecting an isopycnal surface, the velocity structure can be used to define the interface. A layer interface can be defined by identifying the point of the most severe transition in a vertical velocity profile or the peak in the second derivative of velocity, $\partial^2 u/\partial z^2$.

An interface defined in this manner is shown with vertical profiles of the streamwise velocity on Fig. 8, superimposed over the transect-3 cross section from Fig. 4. This estimate of the interface elevation demonstrates a bottom attachment very near the lip of the bathymetry break, as identified in the figure, and coincident with isohalines in the range from 10 to 15 psu. For the determination of the Froude number near the lift-off point, the choice of a layer interface coincident with the 14-psu isohaline surface is consistent with the velocity structure. Although this alternative definition of the layer thickness has a slight effect on the Froude number estimate seaward of the front, it does not change the key finding that the flow is significantly supercritical at the lift-off point. Given the existing velocity structure, the front would have to be pushed downslope to a depth of 14 m in order to produce a Froude number of unity at the lift-off point, as shown in Fig. 8. This downslope location is not consistent with observations.

The observed supercritical Froude numbers are also not reflective of a poor choice for the value of g'. Salinity differences required to generate critical Froude numbers within the frontal zone given the existing ve-

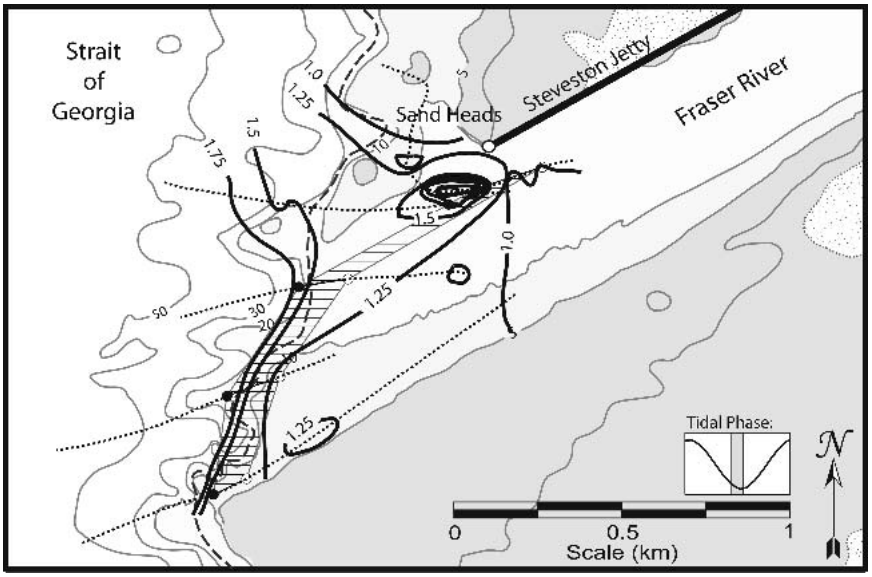

FIG. 7. Upper-layer Froude number across the lift-off zone during the late ebb on 30 Jun 2000. The 14-psu front is defined by the hatched region, and the open and closed circles, which represent definitive locations on the landward and seaward sides of the front, respectively. Contours landward of the front represent "virtual" Froude numbers, estimated using a representative value of g', as shown in Fig. 1. The layer interface was defined as the location of the 14-psu isohaline. Dotted lines represent ship tracks. Dashed line represents the 12-m isobath, as in Fig. 2.

locity profiles would be on the order of an unrealistic 40–60 psu.

b. Bottom friction, velocity shear, and mixing

Hydraulic theory (e.g., Armi and Farmer 1986) is inviscid and cannot account for the effects of boundary layer induced shear or turbulent mixing across the layer interface. These influences have been addressed in several studies that can provide some insight into the role of viscous processes in the present case. Jirka and Arita (1987) argue that the shape of a density intrusion can range from a frictionally controlled wedgelike shape to a hydraulically controlled, blunt-faced profile. Their laboratory experiments further suggested that nonuniformities in the channel bottom, such as bumps or steps, can be sufficient to break up the boundary layer and force the intrusion profile toward the hydraulically controlled state with frictional affects playing only a second-order role.

Gerdes et al. (2002) have investigated the importance of interfacial mixing and entrainment on the hydraulic control of two-layer exchange flows. Their results suggest that these viscous processes result in a downstream shift of the hydraulic control location. Similarly, Garrett and Gerdes (2003) found that shear within a single-layer, uniform-density flow reduced the critical value of the Froude number to a value less than 1 and also shifted the control location in the downstream direction.

In the Fraser River lift off, the shape of the interface appears to resemble the blunt-faced density intrusion described by Jirka and Arita (1987), suggesting that the interface is controlled primarily by inviscid hydraulic processes and that frictional effects are not first order. The steep drop-off in bathymetry and the presence of significant sand waves in the region, with typical heights of order 1 m (Kostaschuk and Luternauer 1989), may be sufficient to break up the local boundary layer effects. This assessment is also consistent with comparisons to Garrett and Gerdes (2003). Although caution must be taken in comparing the uniform-density flow described by Garrett and Gerdes (2003) with the stratified flow present in the Fraser River, such a comparison might suggest that significant shear would force the critical Froude number toward a value less than 1. The observations summarized in Fig. 7 clearly indicate that Froude numbers at the front are greater than 1.

The significance of the Gerdes et al. (2002) results to the case of an arrested front, as observed in the Fraser, is likely to be limited. The region where entrainment and interfacial stress is viable in the arrested-front condition is downstream of the control point, and information from that region presumably cannot propagate upstream to affect the front location. Mixing processes may have some influence at the front itself and are certainly responsible for broadening a spatially isolated front into a frontal zone, defined by the presence of intermediate-salinity fluid. There may also be some "leakage" of dense water landward of the observed lo-

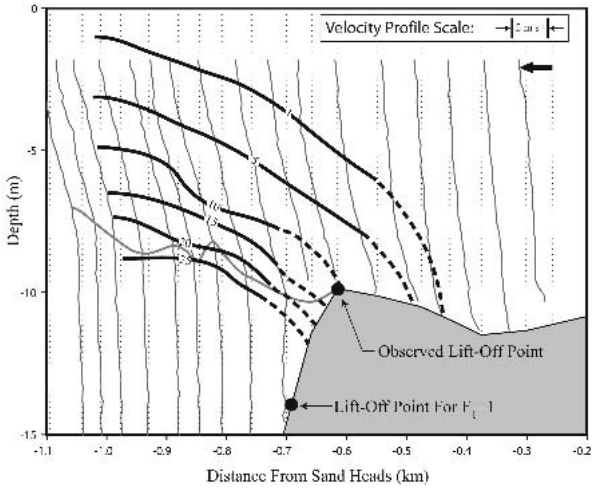

FIG. 8. Streamwise velocity profiles overlaid on the lift-off cross section identified as transect 3 in Fig. 3. The thick gray line represents the interface boundary as defined by a visual assessment of the point of the most abrupt change in the slope of the velocity profiles. At locations where robust velocity data do not extend deep enough, a lowest-case estimate has been made by extrapolating the observable slope to $u = 0$ (dotted lines). The two filled circles indicate the difference between the observed lift-off point, using the visual method just described, and the lift-off point required for a streamwise upper-layer Froude number of 1 (using a vertical mean of the streamwise velocity). To meet the constraint of $F_1 = 1$, a significant deflection of the isohalines near the steeply sloping portion of the bottom would be required.

cation of the front very close to the bottom within the bottom boundary layer, as described by Geyer (1985). Such effects are difficult to detect with the resolution afforded by the tow-yo sampling scheme employed in this study. Any leakage of fluid landward of the front, however, is immediately subject to intense boundary layer shears and is likely mixed upward in the water column fairly quickly. This may be a primary mechanism responsible for broadening the width of the frontal zone.

The role played by viscous effects in modifying the inviscid two-layer hydraulic solutions, described by Armi and Farmer (1986), Farmer and Armi (1986), and others, is still an area of active research with much that is unclear. However, a comparison of the present observations with earlier studies, including loose analogy to the unstratified case described by Garrett and Gerdes (2003), suggests that viscous affects may play a reduced role at the front associated with the Fraser lift off. As such, the remainder of this paper proceeds with an analysis of the observational data within an inviscid framework.

c. Froude angle

The supercritical conditions observed at the front may be reconciled with theory by accounting for an oblique orientation of the front to the oncoming flow. This section examines the critical conditions for an oblique front.

Consider the growth of a wave front emanating from a point of disturbance in a moving flow (e.g., Liggett 1994, 319–323). Under critical flow conditions, the flow velocity matches the wave speed and the upstream edge of the wave front remains fixed at the point of the disturbance as shown in Fig. 9a, while the radius grows with time. Under supercritical conditions, the entire disturbance is swept downstream, but the envelope of information transmittal is not limited to the axis of the flow direction and defined by the difference between the ambient flow velocity and the wave speed, as in the one-dimensional case. Here, as shown in Fig. 9b, the envelope of influence of the disturbance can be identified by the half-angle formed between the direction of the ambient flow and a line emanating from the point of the disturbance tangent to the wave circle at all times. This angle, the Froude angle, is equivalent to the Mach angle from supersonic flow theory (Garvine 1982) and can be defined as

$$\phi = \sin^{-1}(F^{-1}). \tag{4}$$

Ippen (1936) derived this angle for supercritical hydraulic flows and discussed its implications with regard to curved sections of uniform-density open-channel flow. Although Ippen's flow structure was applied to one-layer (free surface) hydraulics, the basic theory is the same: that information can only be propagated within the wedge bounded by the Froude angle to either side. This region, bounded by lines tangent to the expanding wave circle at all times, represents the envelope of all characteristics emanating from the point of disturbance. The Mach angle concept is well established in the fields of compressible fluid dynamics and aerodynamics (e.g., Kundu and Cohen 2001, 694–696) and has led to many innovations in the aviation industry over the last half-century. Its application to hydraulic flows has been investigated in less detail, as evidenced by the limited number of references to this concept in the hydraulic literature, although the idea has been exploited as a numerical technique for obtaining solutions for the propagating front of an advancing river plume in both one (O'Donnell and Garvine 1983) and two dimensions (O'Donnell 1990).

If we now consider a front defined by a line at an arbitrary angle, α, with respect to the ambient flow, as shown in Fig. 9c, the flow will be considered critical with respect to the front as long as information can be transmitted along the front, but not to the upstream side of the front. This is accomplished only when $\phi = \alpha$ so that the front must always be oriented at an angle with respect to the ambient flow equal to the Froude angle. This is equivalent to the expression $F \sin\alpha = 1$, which implies that the Froude number, using the component of velocity perpendicular to the front, is critical in the traditional one-dimensional sense. This interpretation is also shown in Fig. 9c.

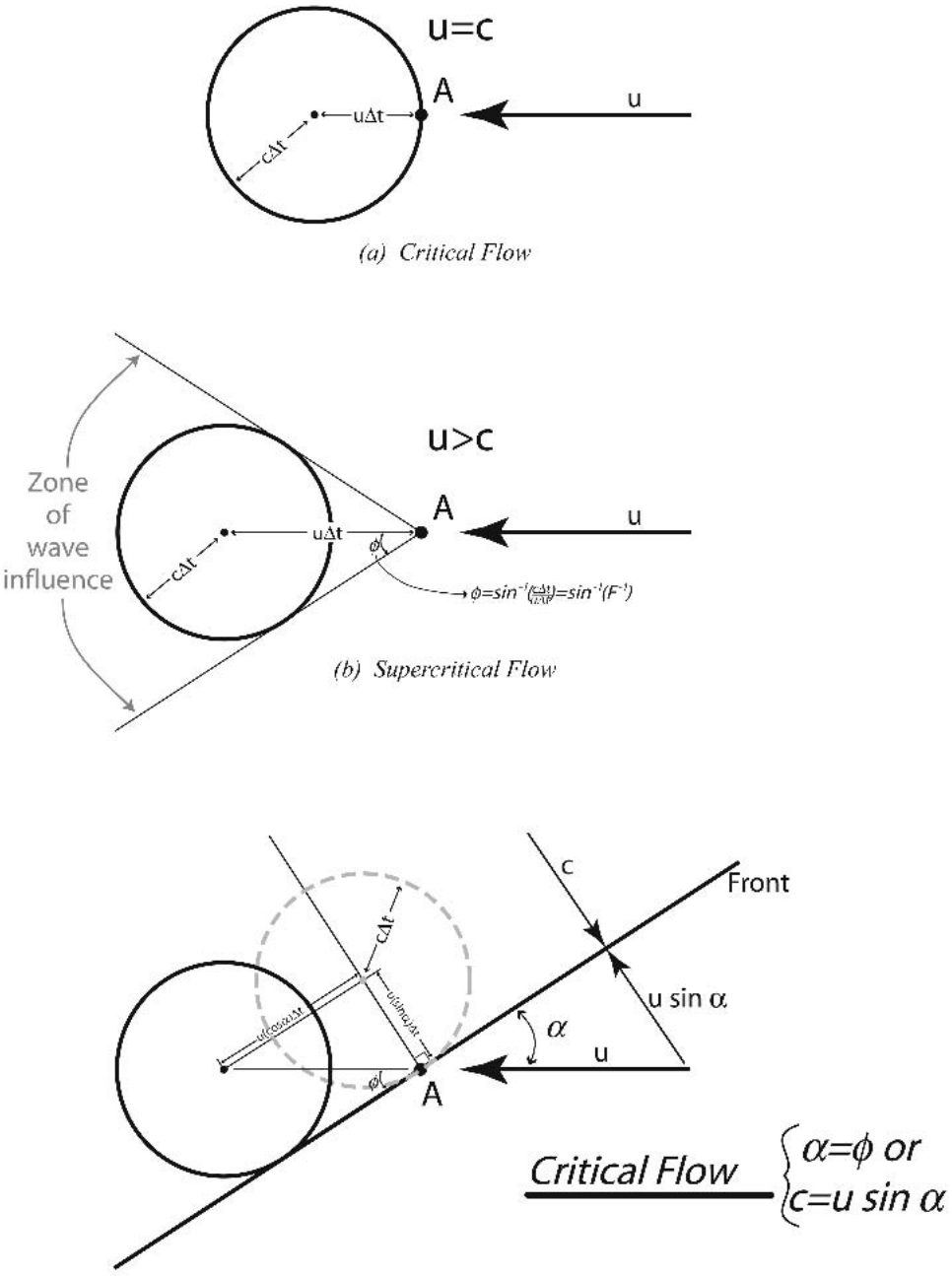

FIG. 9. Propogation of wave fronts for critical and supercritical flow, and critical conditions for an oblique front. In all cases a flow with velocity u flows from right to left, and an instantaneous disturbance is initiated at point A. (a) Critical flow is demonstrated, where the wave speed of the fluid, $c = (g'h)^{1/2}$, is equal to u, and the right-hand edge of the wave field forms a stationary wave at A but propagates to the left elsewhere. (b) In supercritical flow, all portions of the wave front move away from A in the same direction because of the $u > c$ condition. Here the envelope of the wave influence can be described by a Froude angle ϕ, as shown. (c) It is shown how this concept of supercritical flow can represent critical flow relative to a two-dimensional front when the Froude angle is equal to the angle of inclination between the front and the oncoming flow, α. In this case, a Froude number calculated using the velocity component normal to the front, as demonstrated by the dashed representation of the wave front and the velocity components shown perpendicular to the front, is equal to 1, as in the one-dimensional case presented in (a).

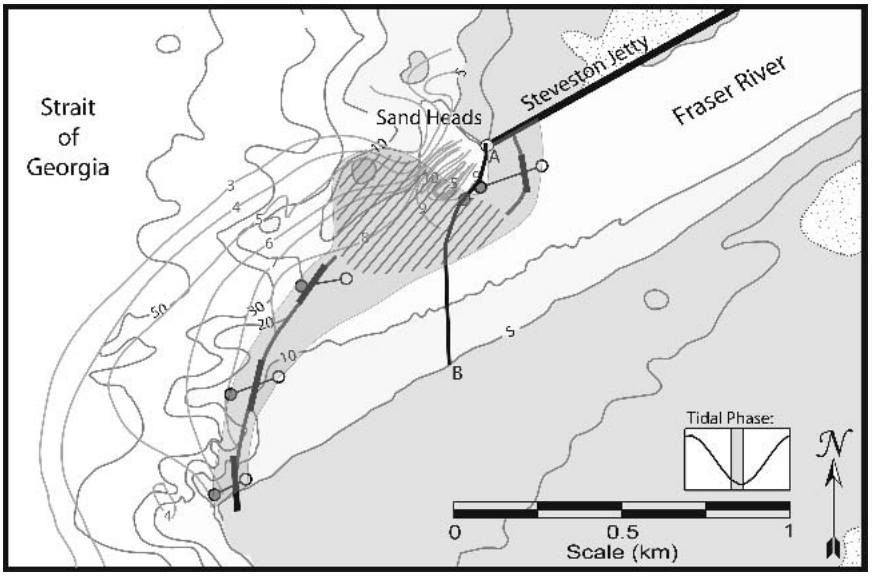

FIG. 10. Froude angle estimates for lift-off region, calculated from the Froude numbers shown in Fig. 7. The calculated Froude angles are shown as the thick black line segments. The shaded region represents conservative limits of the frontal zone (5–20 psu), as based on observational data, and the 14-psu front is identified by the open and closed circles, similar to Fig. 7. The thick gray line is a representation of the front that meets the constraints of both the observed front location and the Froude angle. The hatched area represents a region where the front is not well constrained by the available data. The front in this region may not be well defined, and dominated more by mixing processes and viscous effects than nonlinear inviscid dynamics. Contours represent the depth of the 14-psu isohaline surface. Line segment A–B represents the path of information transfer from Sand Heads across the channel, defined at each point by the local Froude angle.

This concept was tested using the streamwise Froude numbers presented in Fig. 7. The Froude angle was calculated for each Froude number evaluated near the observed front. These angles are shown graphically in Fig. 10, along with the observed front locations for each transect. The Froude angle constraint is clearly consistent with the observations. The only part of the frontal zone in which the theory fails is the hatched area in Fig. 10. The location of the front is poorly constrained by the available data in this region, and the dynamics appear to be more complicated than the hydraulic processes that dominate the rest of the frontal zone.

d. Expansion control versus bottom control

There are two bathymetric features present in the Fraser lift-off zone that may provide the controlling influence on the location of the front: the end of the lateral constraint at Sand Heads, allowing lateral expansion of flow to the north, and the bathymetric break, providing access to the deep water from the Strait of Georgia. These features can generate control mechanisms similar to those described by Armi and Farmer (1986) and Farmer and Armi (1986), respectively. Because the transmittal of information from any point is constrained by the Froude angle, the presence of the expansion at Sand Heads can only influence the front to the extent that it lies within the region defined by a Froude angle path emanating from Sand Heads. An approximation of this path is shown in Fig. 10. In this case, information about the expansion can be transmitted to any point in the region seaward of the defined path. Note that the majority of the frontal zone lies within this region. On the other hand, bathymetric variability provides a local effect, which has the ability to influence the front anywhere along its length.

A qualitative comparison of the cross sections in Fig. 4 to the analytical solutions of Farmer and Armi (1986) suggests that bathymetry may play a role in the location of the frontal zone, as this zone is typically located at the crest or downslope side of the bathymetric break. However, the shape of the interface immediately seaward of the front is not consistent with the Farmer and Armi (1986) solutions, which suggest a flat interface on the seaward side of the crest, but are more similar to the solutions for an expanding channel shown in Armi and Farmer (1986). Perhaps the expansion yields a greater influence over the structure of the lift-off zone than does the bathymetry, but the role of the bathymetry in establishing the location of the lift off cannot be discounted. The lack of an expansion would not preclude the lift off from occurring, perhaps at a very similar location, but it would likely change the shape of the interface through the lift-off region.

The position of the front is effectively controlled by physical processes represented by the Froude number, and changes in the Froude number can be driven by both the expansion and bathymetric influences. The relative importance of these two mechanisms to the value of the local Froude number must vary with position across the channel. The front that exists landward of the line A–B shown in Fig. 10 is controlled only by bathymetric influences, as no information about the expansion can be transmitted to the region. The remainder of the front is likely influenced to some degree by both mechanisms.

5. Implications of Froude angle control and local kinematics

The analyses summarized in Fig. 10 suggest that flow is controlled in the lift-off region not by the Froude number, but by the Froude angle. This results in a significant modification of the constraint on front position relative to the one-dimensional flow situation, indicating that a steady front can occur under supercritical conditions. Although previous data collected from other estuaries (Wright and Coleman 1971; Kashiwamura and Yoshida 1978; Park et al. 1993) has tended to support the one-dimensional theory, indicating that the Froude number is in the vicinity of 1 near the front, this generalization of the critical Froude number concept has significant implications for the dynamics associated with estuarine fronts in many diverse situations.

a. Application of the Froude angle theory

The classical one-dimensional theory represents a limiting case for the Froude angle concept characterized by a front perpendicular to the oncoming flow, $\alpha = 90°$, and a critical "point" where $F = 1$. The upstream extent of any front must conform to this limiting case. The upstream extent of a front may be manifested by an endpoint, as the front intersects a wall or other abrupt transition in bathymetry, in which case the front must reach that endpoint at right angles to the oncoming flow. In other cases, the upstream extent may be created by local symmetry with a portion of the front perpendicular to the oncoming flow, typically at the deepest portion of the channel and the front tailing away at some $\alpha < 90°$ to each side. In either case, there is a region of the front that cannot receive information from upstream along a Froude angle path because no upstream frontal region exists, so the hydraulic control at that point must be locally one dimensional. The existence of a critical Froude number of unity at the front also implies that transport of dense water to the front can be accomplished through upstream-directed flow in the lower layer, creating a classical two-dimensional pattern of estuarine circulation.

At its northern endpoint, the front shown in Fig. 10 is consistent with the limiting case of $\alpha = 90°$, intersecting the Steveston Jetty perpendicular to the channel with a Froude number approximately equal to 1. The dredged channel adjacent to Steveston Jetty is the deepest portion of the channel, so it is consistent that the leading edge of the front should be located there and that the flow should be locally critical in a one-dimensional sense. Given such a point of local one-dimensionality, the position of the front is then established by bathymetric constraints and not by the availability of an upstream source. In the present case, this would imply that the position of the front is independent of the terminus of the Steveston Jetty, and inspection of Figs. 6 and 10 indicates that the intersection of the front with the jetty is, in fact, located upstream from the jetty endpoint.

If the Froude number is greater than 1, then information and mass can only originate from an upstream location. Thus the salt balance in the frontal zone cannot be maintained by a landward, estuarine-type circulation. Rather, the salt balance appears to be accomplished by cross-channel, or along-front, flow. Evidence for this cross-channel propagation of mass within the salt wedge can be seen in Fig. 4, where southward directed velocities on the order of 20–40 cm s^{-1} can be seen immediately below the pycnocline. Mass balance calculations of salt flux within the lift-off zone have shown that the majority of salt is delivered to the front via these cross-channel velocities, and not through a traditional two-dimensional estuarine circulation (MacDonald 2003). As shown in Fig. 9, the along-front component of velocity in the upper layer is equal to $u_1 \cos(\alpha)$, and is on the order of 1 m s^{-1} for the data shown. The along-front flux of saltwater in the lower layer is critical for supplying a mass of saltwater to the region as a replacement for fluid entrained into the advancing upper layer through turbulent mixing processes that occur seaward of the front. However, the velocities in the lower layer need not match the along-front component of the upper-layer flow because the lower-layer flow is driven by the dynamics of the noninviscid mixing processes occurring seaward of the front and, more generally, by the ebbing tide in the Strait of Georgia. The key aspect of the lower-layer flow is that it is in the along-front direction and does not represent a typical two-dimensional estuarine circulation. In a purely inviscid flow, there would be no requirement for lower-layer transport, although a pressure gradient may exist in the lower layer as a result of unmatched barotropic and baroclinic gradients. The magnitude of this lower-layer pressure gradient, however, cannot be constrained by hydraulic theory.

The concept of Froude angle control should be applicable in many different hydraulic control scenarios. Garvine (1982), developed a model for plume expansion that incorporated a similar Froude angle dependence for defining the surface fronts of buoyant plumes. The model was used to predict the location and orientation of the surface front with respect to an am-

bient cross flow and was capable of explaining the structure of the Connecticut River plume front. Surface fronts at convergence zones are often identifiable by lines of debris or foam streaks that are often oblique to the prevailing surface flow direction (Largier 1992) and are likely controlled by Froude angle dynamics.

Bottom-attached fronts with similar orientation to the front observed at the mouth of the Fraser have been predicted analytically and observed in laboratory experiments for buoyant jets discharged over a uniformly sloping bottom (Adams and Stolzenbach 1977). The bottom-attached region in these cases consisted of a long and narrow triangular region with the bottom front emanating into the jet region at an angle from the end of both channel boundaries. The basic geometry of this solution is consistent with the Froude angle theory. Oblique bottom attached fronts have also been observed in several different natural systems. The thermal plume created by the discharge of the Niagara River into Lake Ontario detaches from the bottom in the vicinity of a steep bathymetric break (Masse and Murthy 1990), similar to the Fraser plume. Although Froude number estimates are not available, it is likely that the oblique path of the lift-off follows the Froude angle. An example of Froude angle criticality has been seen within the confines of the estuarine channel in the Hudson River (New York), where angled fronts have been observed at supercritical streamwise Froude numbers (Geyer et al. 1998). These observed angled fronts are driven by significant cross-channel variability in bathymetry within the Hudson channel.

The importance of the Froude angle may also be significant in hydraulic control situations where both layers are active, although two-dimensional observations of these phenomena are scarce. Klymak and Gregg (2001) emphasize the importance of three-dimensional structure to the dynamics of a stratified overflow in Knight Inlet, identifiying lateral recirculations in the lee of the sill. This particular overflow has been well studied along the *thalweg* (Farmer and Armi 1999), with observations that are consistent with the one-dimensional Farmer and Armi (1986) theory. It is possible that conditions observed along the *thalweg* are consistent with the one-dimensional theory because of the local symmetry but that outside of the *thalweg,* where lateral variability has been observed, the location of the control section may be affected by the transmittal of information along oblique wave characteristics, similar to the Fraser Estuary front.

b. Limitations of the Froude angle theory

It was pointed out earlier that there are certain regions where the inviscid nature of the Froude angle theory may not allow an adequate description of the front position. The hatched region in Fig. 10 is such a region. If we follow the front southward from Sand Heads, assuming the shape of the front is defined by the local Froude angle, we might expect it to take a shape similar to the line A–B shown in Fig. 10, which is the Froude angle defined path emanating from Sand Heads. Instead the frontal zone (delineated by the shaded region in Fig. 10) runs approximately parallel to the channel through the hatched region in Fig. 10 until it once again becomes hydraulically controlled and stable near the bathymetric break. Some insight into the nature of this discrepancy may be achieved by examining the Froude number contours of Fig. 7. The broad region of the channel adjacent to the hatched area of Fig. 10 is characterized by relatively constant Froude numbers. A front may stabilize in this region briefly at the beginning of the lift-off period as it retreats from the channel. However, any perturbation in flow rate that briefly increases the local Froude number would drive the front seaward. Upon relaxation of the increase, the salt wedge cannot return landward to its original position because conditions remain critical at the new location. In this manner, the front is ultimately pushed to the edge of the bathymetric break where it encounters a significant Froude number gradient. The front within the hatched region does not appear to be in dynamical balance, based on the steady, inviscid theory. In this region the front is probably maintained by a combination of frictional and transient processes.

6. Conclusions

The Fraser River lift-off is a good example of highly stratified, or two-layer, arrested flow and illustrates many aspects of estuarine fronts common to other physical settings. The steady front that forms outside the mouth of the Fraser during late ebb is controlled by the dynamics associated with the sudden expansion of the channel and local bathymetry. A Froude angle can be defined, which can be interpreted as a rotation of the reference frame, so that the velocity component in the new direction results in a critical value of the Froude number. The alignment of the front is established in response to this local Froude angle so that the velocity component perpendicular to the front is critical. This importance of the Froude angle, as opposed to the Froude number itself, is an intriguing concept that bears further theoretical, numerical, and observational investigation. This concept may well serve as a useful extension of the one-dimensional theory of Armi and Farmer (1986) and Farmer and Armi (1986).

Acknowledgments. The authors thank David Jay, Philip Orton, and Alex Horner for their help during the field efforts. We also appreciate the helpful comments provided by Rich Garvine and an anonymous reviewer. This work was performed as a part of D. MacDonald's Ph.D. thesis, and was funded by Office of Naval Research Grants N000-14-97-10134 and N000-14-97-10566, National Science Foundation Grant OCE-9906787, a National Science Foundation graduate fel-

lowship, and support from the WHOI Academic Programs Office.

APPENDIX

Elliptical Interpolation Scheme

Observed quantities were interpolated across the near-field region using a simple weighted averaging scheme. Assuming a total of N observations of a given quantity (i.e., salinity, velocity, etc.) within a specific depth range, the interpolated value of the quantity at any point in the domain was taken as

$$u = \frac{\sum_{i=1}^{N} (l_i u_i)}{\sum_{i=1}^{N} l_i}, \tag{A1}$$

where

$$l_i = D_i^{-\phi} \quad \text{and} \quad D_i = [M_i^2 + (\gamma m_i)^2]^{1/2}.$$

Here, u represents the quantity of interest, M_i represents the distance between the interpolation point and observation point i along some major axis, and m_i is the distance along a minor axis oriented normal to the M axis. The parameters ϕ and γ are weighting factors for the overall distance D_i and the minor axis distance m_i, respectively. For the interpolations near the Fraser liftoff, we used $\phi = \gamma = 10$, and a major axis oriented at an azimuth of 60°.

REFERENCES

Adams, E. E., and K. D. Stolzenbach, 1977: Analysis of a buoyant surface discharge over a shallow sloping bottom. *Proc. XVII Int. Association of Hydraulic Research (IAHR) Congress,* Baden Baden, Germany, International Association for Hydraulic Research, 363–370.

Armi, L., 1986: The hydraulics of two flowing layers with different densities. *J. Fluid Mech.,* **163,** 27–58.

——, and D. M. Farmer, 1986: Maximal two-layer exchange through a contraction with barotropic net flow. *J. Fluid Mech.,* **164,** 27–51.

——, and ——, 1988: The flow of Atlantic water through the Strait of Gibraltar. *Progress in Oceanography,* Vol. 21, Pergamon, 1–105.

Benjamin, T. B., 1968: Gravity currents and related phenomena. *J. Fluid Mech.,* **31,** 209–248.

Dalziel, S. B., 1991: Two-layer hydraulics: A functional approach. *J. Fluid Mech.,* **223,** 135–163.

Farmer, D. M., and L. Armi, 1986: Maximal two-layer exchange over a sill and through the combination of a sill and contraction with barotropic flow. *J. Fluid Mech.,* **164,** 53–76.

——, and ——, 1988: The flow of Mediterranean water through the Strait of Gibraltar. *Progress in Oceanography,* Vol. 21, Pergamon, 1–105.

——, and ——, 1999: Stratified flow over topography: The role of small-scale entrainment and mixing in flow establishment. *Proc. Roy. Soc. London,* **455A,** 3221–3258.

Garrett, C., and F. Gerdes, 2003: Hydraulic control of homogeneous shear flows. *J. Fluid Mech.,* **475,** 163–172.

Garvine, R. W., 1982: A steady state model for buoyant surface plume hydrodynamics in coastal waters. *Tellus,* **34,** 293–306.

Gerdes, F., C. Garrett, and D. Farmer, 2002: On internal hydraulics with entrainment. *J. Phys. Oceanogr.,* **32**, 1106–1111.

Geyer, W. R., 1985: The time-dependent dynamics of a salt wedge. Ph.D. thesis, University of Washington, 200 pp.

——, and D. M. Farmer, 1989: Tide-induced variation of the dynamics of a salt wedge estuary. *J. Phys. Oceanogr.,* **19,** 1060–1072.

——, R. P. Signell, and G. C. Kineke, 1998: Lateral trapping of sediment in a partially mixed estuary. *Proceedings 8th International Biennial Conference on Physics of Estuaries and Coastal Seas, 1996,* J. Dronkers and M. B. A. M. Scheffers, Eds., Balkema, 115–124.

Henderson, F. M., 1966: *Open Channel Flow*. Macmillan, 522 pp.

Ippen, A. T., 1936: An analytical and experimental study of high velocity flow in curved sections of open channels. Ph.D. thesis, California Institute of Technology.

Jirka, G. H., and M. Arita, 1987: Density currents or density wedges: Boundary-layer influence and control methods. *J. Fluid Mech.,* **177,** 187–206.

Kashiwamura, M., and S. Yoshida, 1978: Outflow dynamics at a river mouth. *Proc. 16th Coastal Engineering Conf.,* Hamburg, West Germany, ASCE, 2925–2944.

Klymak, J. M., and M. C. Gregg, 2001: Three-dimensional nature of flow near a sill. *J. Geophys. Res.,* **106** (C10), 22 295–22 311.

Kostaschuk, R. A., and J. L. Luternauer, 1989: The role of the salt-wedge in sediment resuspension and deposition: Fraser River Estuary, Canada. *J. Coastal Res.,* **5** (1), 93–101.

Kundu, P. K., and I. M. Cohen, 2001: *Fluid Mechanics.* 2d ed. Academic Press, 694–696.

Largier, J. L., 1992: Tidal intrusion fronts. *Estuaries,* **15** (1), 26–39.

Liggett, J. A., 1994: *Fluid Mechanics*. McGraw-Hill, 319–326.

MacDonald, D. G., 2003: Mixing processes and hydraulic control in a highly stratified estuary. Ph.D. thesis, MIT/WHOI, 214 pp.

Masse, A. K., and C. R. Murthy, 1990: Observations of the Niagara River thermal plume (Lake Ontario, North America). *J. Geophys. Res.,* **95** (C9), 16 097–16 109.

O'Donnell, J., 1990: The formation and fate of a river plume: A numerical model. *J. Phys. Oceanogr.,* **20,** 551–569.

——, and R. W. Garvine, 1983: A time dependent two-layer model of buoyant plume dynamics. *Tellus,* **35A,** 73–80.

Park, C., J. Kim, and S. Chang, 1993: The characteristics on the mixing of freshwater in Suyoung Bay. *Bull. Korean Fish. Soc.,* **26,** 353–362.

Wright, L. D., and J. M. Coleman, 1971: Effluent expansion and interfacial mixing in the presence of a salt wedge, Mississippi River Delta. *J. Geophys. Res.,* **76,** 8649–8661.